ANALYSIS OF THE THERMAL PERFORMANCE OF HEAT EXCHANGERS FOR ACTIVE CHILLED BEAM UNITS

Fernando Domínguez Muñoz[(a)], José Luis González Espín[(b)], Alberto Coronas Salcedo[(c)], José Manuel Cejudo López[(d)]

[(a)] Grupo Energética, Escuela de Ingenierías Industriales, Universidad de Málaga, Málaga, 29071, Spain, fdominguezm@uma.es

[(b)] MADEL Air Technical Diffusion S.L., Barcelona, 08013, Spain, jlgonzalezespin@gmail.com

[(c)] Universidad Rovira i Virgili, Tarragona, 43007, Spain, acoronas@urv.cat

[(d)] Grupo Energética, Escuela de Ingenierías Industriales, Universidad de Málaga, Málaga, 29071, Spain, jmcejudo@uma.es

Abstract: *Coils used in active chilled beams (ACB) have some distinctive features compared to conventional coils used in fan-coil units. On the air side, the flow rate of induced air is limited and air velocities are thus much lower than those prevailing in fan-coils. Consequently, most of the correlations available in the open literature to calculate the convection coefficient on the air side are out of range when applied to ACB coils. In addition, the nature of the induction process causes some degree of non-uniformity in the air distribution over the coil. On the liquid side, circuitry can also be distinctive due to space constrains or functional requirements. Some commercial products use one circuit arrangements (all tubes connected in series) with different possible flow paths; two or more circuit schemes are also frequent. In this paper, ongoing research on active chilled beam modeling is presented. A generic numerical model of plate fin-and-tube heat exchanger is briefly described along with a test bench in which several ACB units have been tested. Experimental data for an example coil is used along with the coil model to determine a correlation for the air-side heat transfer. The calibrated numerical model is then used to simulate the coil.*

Keywords: Active chilled beam, ACB, effectiveness-NTU, heat exchanger

1. INTRODUCTION

An active chilled beam (ACB) is a convector with integrated air supply where the induced air passes through a water-cooled fin-and-tube heat exchanger. Most cooling coils are designed to operate in dry regime. To ensure that there is no condensation, the chilled-water supply temperature must be maintained 1ºC or 2ºC above the room dew point, which results in typical chilled water supply temperatures between 14ºC and 18ºC. As a result, the water circuit typically satisfies between 60% and 85% of the sensible load of the space, while the primary air satisfies 100% of the latent load and the rest of the sensible load. The ACB is thus a terminal unit well suited for applications with low to medium internal latent generation.

The coil inside an ACB has some distinctive features compared to conventional water coils. First, the velocity of the induced air flow is quite low. For the case study presented in this paper, the air Reynolds number varies from 220 to 832. Most of this interval is well below the range of validity of the correlations available in the open literature for finned heat exchangers. Second, the circuitry of the water-side can also be unusual due to factors such as space limitations. For example, in the case study presented below, tubes are divided into 2 circuits, with all tubes in the same circuit connected in series. More conventional connection schemes are also used in ACB, but we can find special cases such as the latter.

Detailed models of the thermal behavior of ACBs are needed to analyze and improve their performance, as well as to study condensation–preventing strategies. Previous work on energy modeling of ACB systems have typically used simple empirical models with adjustable parameters that are regressed using experimental or manufacturer catalog data [1-3]. Only Chen [4,5] has published a detailed numerical model

of ACB, which was used to study the effect of the water-side circuitry on the thermal performance of several beams.

The manufacturer MADEL is interested in fully characterizing the thermal performance of its ACB products. This work encompasses testing the different ACB models manufactured by MADEL, developing a comprehensive mathematical model of ACB, and use this model to calibrate the induction process and the air-side convection coefficient for each ACB geometry. In this paper, we show how this work is developing regarding the modeling of the heat exchanger in the ACB. The test bench were the ACBs are being tested is described in Section 2, followed by Section 3 with a short description of the coil numerical model that has been developed. A case study is presented in Section 4, where the numerical model is used to reduce the air-side thermal resistance of an example coil. A Nusselt correlation is proposed for the coil, and the prediction ability of the model is quantified.

2. TEST BENCH

The steady–state capacity of the chilled beams is measured in the test bench of MADEL. The beam is mounted inside a test room (Figures 1 and 2, left side) where a separate system (not represented in the figures) maintains the air temperature and humidity at the desired values. Several probes are installed along the beam to measure the temperatures of the induced air flow (T_r) and the supplied air flow (T_s). The induced air flow rate (m_{sc}) is not directly measured because the air velocities are too low; instead it is indirectly calculated from the energy balance of the beam. The supplied air mass flow rate (m_s) is neither measured, but calculated from the air mass balance of the beam. The primary air is supplied to the beam through a duct coming from a separate air treatment unit that controls temperature (T_{pr}), humidity (R_{pr}) and static pressure (P_{pr}). The volumetric air flow rate of primary air is measured in a nozzle bank (Figures 1 and 2, right side), and the temperature and static pressure of the primary air are measured before entering the beam. Regarding the water circuit, a water plant controls the temperature of water supplied to the beam. The water volumetric flow rate (V_w) is measured with a magnetic flow meter. Inlet and outlet water temperatures (T_{wi}, T_{wo}) are also measured. Measurement uncertainties, for a coverage factor of 2, are listed in Table 1 for the conditions of the case study described in Section 4.

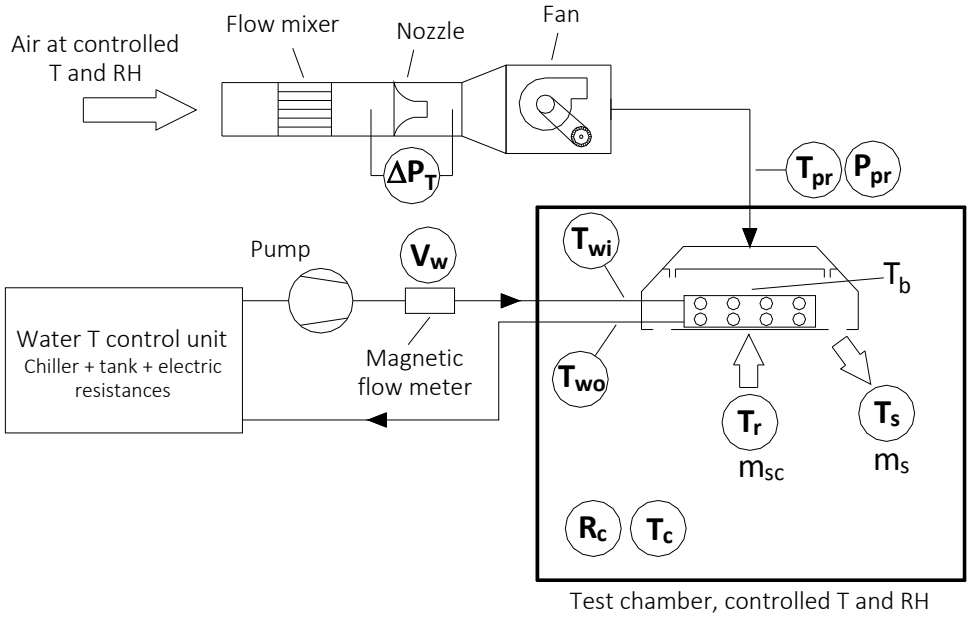

Figure 1. Variables measured during the test

Table 1. Measurement uncertainties (2σ)

Variable	**U (2σ level)**
Temperature	± 0,15 K
Liquid flowrate (V_w)	± 1,65 liter/h
Pressure difference (ΔP_T)	± 2,5 Pa

Figure 2. Chilled beam in the test chamber (left) and nozzle bank for air flow measurement (right)

3. NUMERICAL MODEL

A numerical model of plate−fin−tube heat exchanger has been developed to analyse the thermal performance of the coils used in the ACB units. The were several reasons for developing this model instead of using the simpler, yet accurate and convenient, effectiveness−NTU method [4]: (**1**) there are no ε-NTU equations for some of the water-side circuiting schemes used in chilled beams; the case study in Section 4 is an example of that; (**2**) the induced air flow is non−uniform over the surface of the coil, and we wish to consider and analyse this effect in the future; (**3**) a dynamic coil model will be needed to study control strategies. The ε−NTU method assumes steady−state conditions and uniform flow distribution, so it does not fit the requirements.

A very short description of the steady−state numerical model follows. The user must provide the main geometric dimensions of the coil (see an example in Table 2) and a connectivity matrix describing how the tubes are connected on each circuit. The model divides each tube in N (user−selectable) non−overlapping cells along the tube axis. Each cell is treated as a single cross−flow heat exchanger. The air across the finned segment is assumed to be the unmixed fluid, while the water in the tube is the mixed fluid. In case of condensation, it is assumed that *Lewis* = 1 and the enthalpy difference is used as the driving potential for the total energy flow. The connectivity matrix is used to identify the predecessor and successor cells on the water−side, thus obtaining the ordered sequences of cells through which the water of each circuit flows from the inlet to the outlet. Air−side and water−side balances are numerically iterated until convergence, which is checked by monitoring the outlet temperature and humidity of each cell. Regarding fin modelling, each cell is treated as a discrete unit of heat transfer, not considering the conduction heat transfer through the fin plates between tubes. Fin efficiency is calculated using the approximate Schmidt equation [6]. On the air side, the air flow rate distribution across the heat exchanger is kept the same from the inlet to the outlet. In case of staggered tube arrangements, the inlet temperature and humidity to one internal cell (behind the frontal face) is calculated by mixing the flows coming from the two adjacent cells just below. The water−side convection coefficient is calculated using well known correlations [7], and linearly interpolating the Nusselt number in the flow transition region. Several correlations are implemented to calculate the air−side convection coefficient, along with a generic user−defined correlation of the form:

$$Nu_{air} = C\,\mathrm{Re}_{air}^{n}\,Pr_{air}^{m} \tag{1}$$

Experimental data will be used in Section 4 to identify the parameters in Equation (1) for a particular ACB. The model was implemented in Fortran 2003 and linked to Matlab for easy use (the model along with an interface were compiled as a Matlab MEX file).

4. CASE STUDY

The thermal performance of a particular coil is analysed in this Section: the coil is described (§4.1) and tested (§4.2), the model is then used to calculate the adjustable parameters in Equation (1) (§4.3), and finally the prediction ability of the resulting numerical model is quantified (§4.4).

4.1. Coil characteristics

The relevant characteristics of the example coil are summarized in Table 2. This particular coil is designed to be used in 4−pipe systems. The 24 tubes are divided in 18 tubes for the cooling circuit and 6 tubes for the heating circuit, connected as shown in Figure 3. Tubes are arranged in-line to minimize pressure losses.

Table 2. Coil characteristics

Model (manufacturer code)	WAAB 600 4 WAY C4T
Number of rows in the direction of the air flow	2
Number of tubes per row	12
Number of circuits	2
Fin type	Flat
Fin material	Aluminium
Fin width (normal to air flow)	420 mm
Fin lenght (direction of air flow)	70 mm
Fin thickness	0.12 mm
Fin pitch (including fin thickness)	3 mm
Tube arrangement	Line
Tube material	Copper
Tube lenght	948 mm
Inner diameter of tubes	12 mm
Outer diameter of tubes	12.7mm
Longitudinal tube pitch (S_L)	35 mm
Transversal tube pitch (S_T)	35 mm

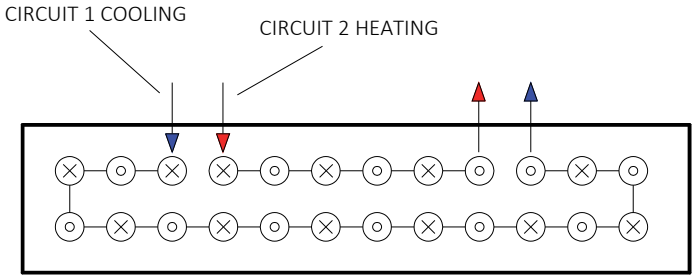

Figure 3. Tube connections in the coil WAAB 600 4WAT C4T

4.2. Measurements

The coil was mounted in the test room. Tests were performed for different primary air flow rates, maintaining essentially constant the remaining inlet variables (T_{wi}, V_w, T_{pr}). Measurements are performed under steady state conditions, which are considered to have been obtained when the standard deviations of the recorded measurements (sampling rate approximately 1 per minute) are within the limits given in the standard UNE EN-15116 [8]: ± 0.05 K for T_r, ± 0.05 K for T_{wi} and T_{wo}, 1% of nominal for V_w, 1.5% for V_{pr}, and ± 0.2 K for T_{pr}.

Table 3 shows the results of 12 different tests (nomenclature in Figure 1). The uncertainty in these measurements is given in Table 1. The information in Table 3 can be easily processed to derive the quantities shown in Table 4. The primary air mass flow rate can be calculated from the differential pressure ΔP_T using the discharge coefficient k_T of the nozzle and the air density:

$$m_{pr} = \rho_{pr} k_T \sqrt{\Delta P_T} \tag{2}$$

The capacity of the coil can be calculated from the water energy balance:

$$Q_w = V_w \rho_w c_{p,w} \left(T_{w,o} - T_{w,i} \right) \tag{3}$$

Where $c_{p,w}$ is evaluated at the average water temperature. The induced air flow rate is calculated from the following energy balance to the air:

$$\dot{m}_{pr} h_{pr} + \dot{m}_{sc} h_r = \left(\dot{m}_{pr} + \dot{m}_{sc}\right) h_s = \dot{m}_s h_s \,, \tag{4}$$

where h is the enthalpy at the corresponding temperature and pressure. The result of these calculations along with the propagated uncertainties are shown in Table 4.

Table 3. Measured variables (steady state)

CASE	T_{wi} (ºC)	T_{wo} (ºC)	V_w (liter/h)	T_r (ºC)	T_s (ºC)	T_{pr} (ºC)	ΔP_T (Pa)	k_T
1	16.00	21.17	170	25.98	22.41	23.61	276.2	13.76
2	15.97	20.64	170	26.02	21.98	23.43	183.7	13.77
3	15.99	19.85	170	25.98	21.26	22.70	297.3	7.918
4	15.96	18.98	170	25.98	20.61	22.02	161.0	7.917
5	16.02	20.65	170	25.99	21.64	23.03	316.5	7.923
6	16.03	19.95	170	26.02	20.94	22.01	192.1	7.917
7	16.02	19.38	170	26.02	20.52	21.65	128.2	7.935
8	16.02	18.53	170	26.05	20.09	21.44	68.62	7.921
9	16.02	20.20	170	25.99	21.43	23.30	148.1	7.932
10	15.97	19.76	170	26.04	21.00	22.20	109.3	7.923
11	15.98	19.21	170	26.03	20.69	21.92	74.08	7.928
12	16.03	18.21	170	26.03	20.33	21.67	33.49	7.884

Table 4. Derived quantities

CASE	m_{pr} (kg/s)	m_s (kg/s)	m_w (kg/s)	Qw (W)
1	0,07554 ± 0,0002762	0,2843 ± 0,02059	0,04715 ± 0,0002358	1019,74 ± 42,15
2	0,06170 ± 0,0003374	0,2270 ± 0,01580	0,04715 ± 0,0002358	921,17 ± 42,10
3	0,04525 ± 0,0001539	0,1606 ± 0,01143	0,04716 ± 0,0002358	761,46 ± 42,02
4	0,03337 ± 0,0002080	0,1105 ± 0,00892	0,04716 ± 0,0002358	595,81 ± 41,96
5	0,04667 ± 0,0001493	0,2090 ± 0,01403	0,04715 ± 0,0002358	913,27 ± 42,09
6	0,03645 ± 0,0001906	0,1515 ± 0,01039	0,04716 ± 0,0002358	773,28 ± 42,02
7	0,02988 ± 0,0002336	0,1200 ± 0,00890	0,04716 ± 0,0002358	662,85 ± 41,98
8	0,02184 ± 0,0003185	0,0827 ± 0,00760	0,04716 ± 0,0002358	495,21 ± 41,93
9	0,03193 ± 0,0002162	0,1800 ± 0,01243	0,04716 ± 0,0002358	824,55 ± 42,05
10	0,02750 ± 0,0002520	0,1477 ± 0,01037	0,04716 ± 0,0002358	747,66 ± 42,01
11	0,02268 ± 0,0003063	0,1188 ± 0,00914	0,04716 ± 0,0002358	637,22 ± 41,97
12	0,01517 ± 0,0004532	0,0751 ± 0,00784	0,04717 ± 0,0002358	430,12 ± 41,91

4.3. Air-side convection correlation

The coefficients in Equation (1) can be reduced from the data in Tables 2, 3 and 4 using the numerical coil model. To this aim, a computer program was prepared that calculates, for each test point, the value of Nu_{air} that minimizes the difference between the cooling capacity calculated by the model and measured in the test. The results are then least-squared fitted to the function (1) in order to calculate C and n. The result for the considered coil is:

$$Nu_{air} = 0.08754 Re_{air}^{0.7504} Pr_{air}^{0.3} \tag{5}$$

The collar diameter was used as characteristic length in the Nusselt and Reynolds numbers. The 95% confidence bands for the fitted parameters are: $C \in [0.00875, 0.1663]$ and $n \in [0.6068, 0.894]$. Function (5) along with the elemental points used in the regression are shown in Figure 4.

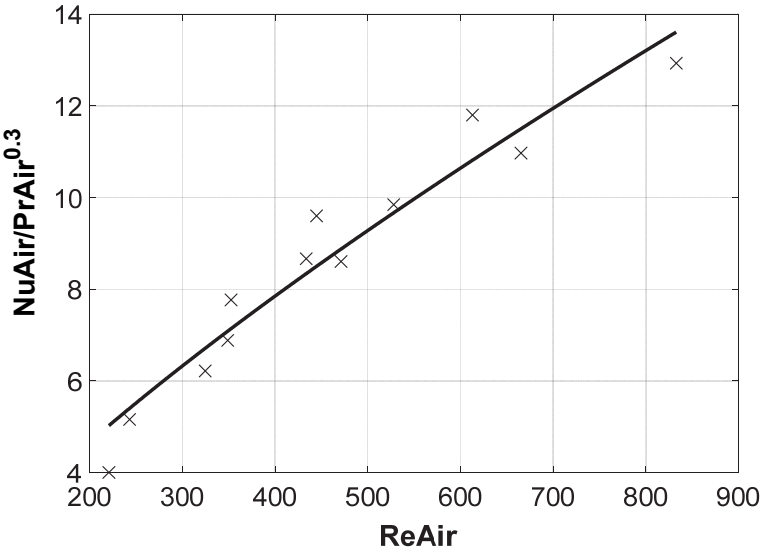

Figure 4. Regression of the Nusselt air-side correlation

In the previous calculation we have assumed that the model is good enough in describing all the physical phenomena that take place in the coil except the air convection, which is used as a freely adjustable parameter to fit the model response to the experimental results. The calculated coefficients are quite reasonable, although the exponent is somewhat larger than normal for the air-side. Its value should be around 0,6 for laminar flow.

4.4. Prediction ability of the model

Now the fitted correlation (5) is introduced in the model and the model is used to calculate the cooling capacity of the coil at the points of Table 3. The results are shown in Figure 5.

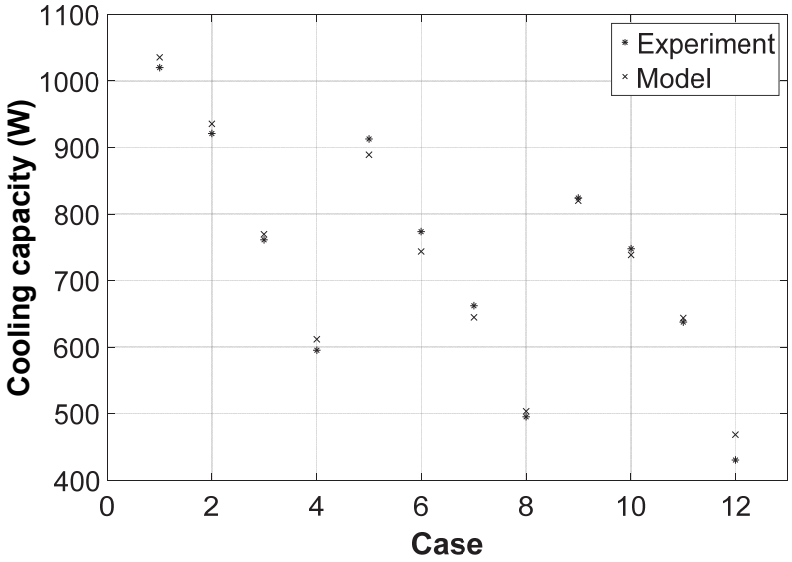

Figure 5. Model-calculated cooling capacity using the correlation (5)

The maximum relative error is 8% for test point number 12.

5. CONCLUSIONS

This paper has summarized ongoing research on active chilled beam modeling. All ACBs of the manufacturer MADEL are being tested and their induction and heat−transfer characteristics correlated. In this paper, an example coil has been analyzed to illustrate the procedure. Steady-state experimental data was used along with a numerical coil model to reduce the air-side thermal resistance, which was then correlated as a function of the Reynolds number. The resulting model predicts the performance of the coil with

reasonable accuracy, and is being used to better understand important questions such as the water circuit design. There are still many open questions that need to be investigated, for example, the effect of non-uniformities in the air flow or the reason why the exponent in Equation (5) is larger than expected.

REFERENCES

[1] Filipsson P, Trüschel A, Gräslund J, Dalenbäck J. A thermal model of an active chilled beam. Energy and Buildings, 2017, 149: 83 – 90

[2] Maccarini A, Hultmark G, Vorre A, Afshari A, Bergsøe NC. Modeling of active beam units with modelica. Building Simulation, Oct 2015, 8(5): 543–550

[3] EnergyPlus Department of Energy (DOE). Web. https://energyplus.net// (accessed January 15th 2018)

[4] Chen C, Cai W, Wang Y, Lin C. Performance comparison of heat exchangers with different circuitry arrangements for active chilled beam applications. Energy and Buildings, 2014, 79:164-172

[5] Chen C, Cai W, Wang Y, Lin C. Further study on the heat exchanger circuitry arrangement for an active chilled beam terminal unit. Energy and Buildings, 2015, 103: 352 – 364

[6] McQuiston FC, Parker JD, Spitler JD. Heating, Ventilating and Air Conditioning. Analysis and Design. John Wiley and Sons, USA, 2000

[7] Verein Deutscher Ingenieure, VDI-Gesellschaft Verfahrenstechnik und Chemieingenieurwesen. VDI Heat Atlas, Chapter G1. Springer-Verlag, 2010

[8] AENOR. Norma UNE EN-15116:2008, Ventilación de edificios. Vigas frías. Ensayo y evaluación de las vigas frías activas.